American Mineralogist, Volume 58, pages 577–587, 1973

High-Temperature Crystal Chemistry of Hortonolite

GORDON E. BROWN,[1] AND C. T. PREWITT

Department of Earth and Space Sciences, State University of New York, Stony Brook, New York 11790

Abstract

The crystal structure of a hortonolite (Fa_{33}) from lunar rock 12052 has been refined from intensity data collected at 24°, 375° and 710°C. Significant ordering of Fe^{2+} on $M(1)$ was detected [$K_D = 1.19(3)$] and did not change over the temperature range studied. Mean M–O distances and octahedral volumes increase linearly from 24°–710°C whereas mean tetrahedral distances and volumes show no significant changes. Octahedral distortions increase differentially as a function of temperature with $M(1)$ distortion increasing at a faster rate than $M(2)$ distortion. A consideration of these distortions over the temperature range studied helps in understanding recent Mössbauer spectra of olivines as well as the observed relative enrichment of Fe^{2+} on the $M(1)$ site in some olivines.

Structural refinements of another lunar olivine (Fa_{18}) from rock 12018 and a terrestrial metamorphic olivine (Fa_{39}) show them to be significantly ordered [$K_D = 1.15(3)$] and disordered [$K_D = 1.02(4)$], respectively. However, the X-ray site populations for 12018 olivine disclose considerably less ordering [$K_D = 1.15(3)$] than that [$K_D = 1.75$] determined by Virgo and Hafner (1972) using Mössbauer spectroscopy on a more Fe-rich olivine also from lunar rock 12018. This suggests that the earlier-crystallizing Mg-rich olivines are less ordered than the later-crystallizing Fe-rich olivines.

Introduction

The Fe-Mg olivines have received wide mineralogical attention over the past decade because of their obvious geological and geophysical importance. In spite of earlier efforts by Belov, Belova, Andrianov, and Smirnova (1951) the olivine structure was not precisely characterized until the investigations by Hanke (1965) and Birle, Gibbs, Moore, and Smith (1968) yielded accurate atomic coordinates and reasonable estimates of apparent atomic thermal motion. The most surprising result of these modern structural studies of intermediate members along the forsterite-fayalite join is the lack of evidence for ordering of Fe and Mg on the two non-equivalent octahedral sites [$M(1)$ and $M(2)$]. With the development of a direct site refinement technique involving explicit chemical constraints (Finger, 1969), detection of relatively small degrees of ordering of two cations between two sites is now possible using precise X-ray intensity data. Application of this technique to several intermediate Fe-Mg olivines (Finger, 1971; Finger and Virgo, 1971) has shown that olivines may be slightly ordered and, surprisingly, that the larger Fe cation apparently preferentially occupies the smaller $M(1)$ site. These findings based on X-ray data are supported by Mössbauer studies (Bush, Virgo, and Hafner, 1970; Finger and Virgo, 1971; Virgo and Hafner, 1972) but conflict with the somewhat inconclusive results of Burns (1970a) based on crystal field spectra.

The absence or small degree of ordering in Fe-Mg olivines is poorly understood in terms of the various ordering criteria such as size arguments and crystal field effects which are commonly applied to silicates. A major source of uncertainty in applying these criteria is a lack of knowledge of silicate structures over the temperature range (>500°C) where significant diffusion of Fe and Mg occurs. Thermal expansion data alone gives little or no information about differential polyhedral expansions in silicates. However, recent advances in high temperature crystallography—as evidenced by the contributions to this special issue of *American Mineralogist*—have made the collection of intensity data from single crystals at temperatures up to ~1100°C almost routine. Subsequent refinement provides the details of a structure at temperatures which may aid in rationalizing a num-

[1] Present address: Department of Geology, Stanford University, Stanford, California 94305.

ber of mineralogical properties including cation ordering.

The present study of the structure of an intermediate Fe-Mg olivine at several temperatures was undertaken with the hope of rationalizing the observed anti-ordering of Fe and Mg at the atomistic level. In addition the structures of two other Fe-Mg olivines—one lunar and one metamorphic—have been refined using room temperature data in order to characterize their structural states. These results were presented orally at the AGU sponsored Petrologic Crystal Chemistry Conference held at Martha's Vineyard, Massachusetts, in September, 1971.

Experimental Details

Two lunar olivines and a terrestrial metamorphic olivine were selected for study. One of the lunar olivines was handpicked from basalt chip 12052,68. Earlier studies of rock 12052 (Bence *et al,* 1970; Papike *et al,* 1971; Bence *et al,* 1971) suggest that olivine and pigeonite phenocrysts precipitated during an early relatively slow cooling stage, possibly in the lunar interior, followed by a late rapid cooling stage from high temperature at or near the lunar surface. The olivines occur as 0.1 to ~1.5 mm yellowish-brown, euhedral crystals of composition Fa_{31}. Microprobe analysis of the crystal used in this study shows no significant chemical inhomogeneities. A small amount of Al was detected and verified by a second probe analysis. The averaged results of five analyses at different points on the crystal are listed in Table 1. Microprobe analyses of olivines from rock 12052, reported by Bell (1971), show higher weight percent SiO_2 and MgO than our crystal but roughly the same amounts of FeO, CaO and Cr_2O_3. In addition Bell detected ~0.03 percent MnO or ~0.01 Mn per formula unit. Our crystal was not checked for Mn. The abnormally high chromium content (~0.01 Cr per formula unit) of 12052 olivines was interpreted by Bell (1971) to indicate that these olivines crystallized under extremely reducing conditions. He also suggests that the chromium is Cr^{2+} rather than Cr^{3+} by analogy with earlier studies of Apollo 11 olivines.

After the foregoing analyses, the crystal, measuring approximately 0.12 mm on a side, was removed from the probe mount, examined optically and with precession photography, and found to be suitable for further data collection.

Interest in olivines from lunar basalt chip 12018,35 was aroused because the Mössbauer results of Virgo and Hafner (1972) indicated the highest degree of Fe/Mg ordering yet reported in Fe-Mg olivines. Several single crystals from the coarse fraction separate were kindly supplied by Dr. David Virgo (Geophysical Lab). Optical examination showed them to contain minor opaque inclusions. Probe analysis of the crystal chosen for this study gave the composition Fa_{18} and showed negligible inhomogeneities (see Table 1). These results differ considerably from the composition Fa_{66} obtained by Virgo and Hafner (1972) on the fine fraction separate. However, an earlier study of olivines from rock 12018 by Kushiro

TABLE 1. Olivine Chemical Analyses

	OXIDES TOTALS		
Oxide	12018,35	0G2B	12052
SiO_2	38.35	36.74	36.70
MgO	43.74	35.97	35.03
FeO	16.92	26.57	26.87
CaO	0.36	0.03	0.31
Al_2O_3	0.42	0.41	0.42
Cr_2O_3	0.03	0.01	0.43
TiO_2	0.02	0.02	0.06
Total	99.84	99.75	99.82
	NUMBER OF ATOMS PER 4 OXYGENS		
Si	0.978(8)*	0.979(7)	0.980(7)
Mg	1.658(14)	1.428(8)	1.394(12)
Fe^{2+}	0.360(4)	0.594(6)	0.601(4)
Ca	0.010(1)	0.001(1)	0.009(1)
Al	0.012	0.013	0.013
Cr^{2+}	0.001	—	0.009
Ti^{4+}	—	—	0.001
	MOLECULAR PERCENT END MEMBER		
Fo	82.0	71.0	69.5
Fa	18.0	29.0	30.5
	FORMULAE NORMALIZED TO 3 CATIONS		
12018	$(Mg_{1.64}Fe_{0.35}Ca_{0.01})\ (Si_{0.99}Al_{0.01})O_4$		
0G2B	$(Mg_{1.42}Fe_{0.58})\ (Si_{0.99}Al_{0.01})O_4$		
12052	$(Mg_{1.38}Fe_{0.60}Ca_{0.01}Cr_{0.01})\ (Si_{0.99}Al_{0.01})O_4$		

*Numbers in parentheses are estimated standard errors (1$\hat{\sigma}$) based on counting statistics and refer to the last decimal place.

TABLE 2. Cell Parameters and Thermal Expansion*

	12018 (24° C)	0G2B (24° C)	12052 (24° C)	12052 (375° C)	12052 (710° C)	%Expansion (710° C)
a	4.771(4)	4.775(1)	4.785(2)	4.795(2)	4.805(1)	0.42
b	10.274(3)	10.280(1)	10.298(6)	10.337(5)	10.366(3)	0.76
c	6.011(5)	6.016(1)	6.028(1)	6.045(3)	6.068(1)	0.66
V	294.64(26)	295.31(8)	297.04(12)	299.63(15)	302.26(8)	1.76

*Numbers in parentheses represent estimated standard errors (1$\hat{\sigma}$) and refer to the last decimal place quoted.

et al (1971) indicates compositional variations ranging from Fa_{27} to Fa_{57} and shows evidence of magmatic differentiation caused mainly by the settling of olivine. The Mössbauer study of Virgo and Hafner provides no evidence for the presence of Fe^{3+}.

The third crystal used in this study comes from an ultramafic pod within the Partridge Formation—a metamorphosed black shale of middle Ordovician age near South Athol, Massachusetts. The metamorphic grade corresponds to the sillimanite-muscovite zone (650°C-6 kbar) and cooling is thought to have occurred over at least a 100 m.y. period (Peter Robinson, Univ. Massachusetts, personal communication). It was hoped that the very slow rate of cooling would eliminate any possible kinetic problems that may be inherent in cation ordering in olivines. The probe results for this crystal, hereafter referred to as OG2B, are also listed in Table 1 and indicate the composition Fa_{29}.

The chemical formulae used in all subsequent calculations were first normalized to four oxygens and then to three cations. The 0.01 Al per formula unit in each olivine was somewhat arbitrarily assigned to the tetrahedral site. However, in order to aid in valence balance the aluminum might be equally divided between octahedral and tetrahedral sites.

Cell parameters for 12018 olivine and the metamorphic olivine were determined from zero-level precession photographs exposed on quartz-calibrated precession cameras. The estimated errors listed in Table 2 refer to precision of measurement only. The estimated volume errors were computed using the propagation of error technique without any covariance terms. The cell parameters of 12052 olivine at 24°C were determined by measuring the 2θ values of 12 reflections on the Picker diffractometer followed by least-squares refinement.

Approximately 650 non-zero independent intensity data over the range 1–70°2θ were collected at room temperature for each of the three crystals on the automated Picker diffractometer in the Stony Brook Petrologic Crystal Chemistry Laboratory. All data were collected in the $\omega - 2\theta$ mode employing a graphite monochromator, MoKα radiation, a scan

TABLE 3. Parameters for Five Olivine Refinements

	12018 (24° C)	0G2B (24° C)	12052 (24° C)	12052 (375° C)	12052 (710° C)
Number of Observations:					
Per Refinement	665	656	640	649	640
Rejected	0	1	4	2	1
R*	0.023	0.029	0.025	0.031	0.057
R(wt.)**	0.029	0.037	0.032	0.037	0.064
Standard Deviation of a Unit Weight Observation	3.30	2.77	4.89	4.71	6.30
Type of Weights	UNIT	UNIT	UNIT	UNIT	UNIT
Extinction Correction***	$0.306(9)\times10^{-4}$	$0.23(1)\times10^{-4}$	$0.21(2)\times10^{-4}$	$0.31(1)\times10^{-4}$	$0.37(2)\times10^{-4}$

*$R = \Sigma \; ||Fo| - |Fc|| \; / \Sigma |Fo|$

**$R(wt.) = [\Sigma \, w(|Fo| - |Fc|)^2 / \Sigma w Fo^2]^{1/2}$

***Numbers in parentheses represent estimated standard errors (1$\hat{\sigma}$) and refer to the last decimal place quoted.

TABLE 4. Comparison of Positional and Thermal Parameters* of 12018 Olivine (24°C), OG2B Olivine (24°C), and 12052 Olivine (24°C, 375°C, and 710°C)

		12018 Olivine (24°C)	OG2B Olivine (24°C)	12052 Olivine (24°C)	(375°C)	(710°C)
M1	Mg	0.814(2)**	0.708(3)	0.675(3)	0.677(3)	0.670(5)
	Fe	0.186	0.292	+0.325	0.323	0.330
	x	0.0	0.0	0.0	0.0	0.0
	y	0.0	0.0	0.0	0.0	0.0
	z	0.0	0.0	0.0	0.0	0.0
	β_{11}	0.0027(2)	0.0025(2)	0.0036(2)	0.0084(3)	0.0111(5)
	β_{22}	0.0012(1)	0.0013(1)	0.0009(1)	0.0025(1)	0.0045(1)
	β_{33}	0.0027(1)	0.0022(2)	0.0026(3)	0.0053(2)	0.0093(4)
	β_{12}	0.0000(1)	0.0001(1)	-0.0000(1)	-0.0001(1)	-0.0002(2)
	β_{13}	-0.0004(1)	-0.0002(1)	-0.0004(1)	-0.0010(2)	-0.0015(3)
	β_{23}	-0.0004(1)	-0.0005(1)	-0.0004(1)	-0.0010(1)	-0.0017(2)
	***Beq	0.38(1)	0.37(2)	0.36(2)	0.87(2)	1.44(3)
M2	Mg	0.826	0.712	0.705	0.703	0.710
	Fe	0.164	0.288	0.285	0.287	0.280
	Ca	0.010	0.0	0.010	0.010	0.010
	x	0.9888(1)	0.9880(2)	0.9877(1)	0.9886(2)	0.9892(3)
	y	0.2778(1)	0.2782(1)	0.2783(1)	0.2788(1)	0.2792(1)
	z	0.25	0.25	0.25	0.25	0.25
	β_{11}	0.0044(2)	0.0045(3)	0.0053(2)	0.0112(3)	0.0146(5)
	β_{22}	0.0007(1)	0.0009(1)	0.0003(1)	0.0013(1)	0.0027(1)
	β_{33}	0.0030(1)	0.0026(2)	0.0028(3)	0.0060(2)	0.0103(4)
	β_{12}	0.0001(1)	0.0002(1)	0.0001(1)	0.0001(1)	0.0001(2)
	Beq	0.38(1)	0.38(2)	0.34(2)	0.82(2)	1.34(3)
Si	x	0.4270(1)	0.4275(2)	0.4276(1)	0.4279(2)	0.4274(3)
	y	0.0946(1)	0.0950(1)	0.0952(1)	0.0952(1)	0.0950(1)
	z	0.25	0.25	0.25	0.25	0.25
	β_{11}	0.0021(2)	0.0019(3)	0.0027(2)	0.0052(3)	0.0069(4)
	β_{22}	0.0008(1)	0.0008(1)	0.0005(1)	0.0012(1)	0.0024(1)
	β_{33}	0.0028(1)	0.0023(2)	0.0029(3)	0.0050(2)	0.0081(4)
	β_{12}	0.0001(1)	0.0001(1)	0.0001(6)	0.0001(1)	0.0001(2)
	Beq	0.31(1)	0.29(1)	0.29(2)	0.58(1)	0.95(3)
O(1)	x	0.7661(3)	0.7666(4)	0.7659(3)	0.7654(4)	0.7650(8)
	y	0.0918(1)	0.0919(2)	0.0920(1)	0.0919(2)	0.0925(4)
	z	0.25	0.25	0.25	0.25	0.25
	β_{11}	0.0029(4)	0.0030(6)	0.0036(4)	0.0048(6)	0.0074(11)
	β_{22}	0.0014(1)	0.0016(2)	0.0009(1)	0.0027(2)	0.0036(3)
	β_{33}	0.0038(3)	0.0034(4)	0.0041(7)	0.0064(4)	0.0124(10)
	β_{12}	0.0002(2)	0.0003(3)	0.0001(2)	0.0006(3)	0.0009(5)
	Beq	0.46(2)	0.48(3)	0.44(3)	0.84(3)	1.35(6)
O(2)	x	0.2194(3)	0.2179(4)	0.2181(3)	0.2177(5)	0.2169(8)
	y	0.4482(1)	0.4489(2)	0.4493(1)	0.4496(2)	0.4507(4)
	z	0.25	0.25	0.25	0.25	0.25
	β_{11}	0.0041(5)	0.0049(7)	0.0057(5)	0.0111(7)	0.0119(13)
	β_{22}	0.0010(1)	0.0010(1)	0.0005(1)	0.0012(1)	0.0032(3)
	β_{33}	0.0040(3)	0.0033(4)	0.0036(7)	0.0070(5)	0.0101(9)
	β_{12}	-0.0000(2)	-0.0004(3)	0.0002(2)	-0.0003(3)	-0.0001(5)
	Beq	0.45(2)	0.46(3)	0.42(3)	0.86(3)	1.32(6)
O(3)	x	0.2795(2)	0.2806(3)	0.2809(2)	0.2816(3)	0.2829(6)
	y	0.1634(1)	0.1638(1)	0.1637(1)	0.1636(1)	0.1636(3)
	z	0.0336(2)	0.0340(2)	0.0340(3)	0.0348(3)	0.0357(5)
	β_{11}	0.0046(3)	0.0041(5)	0.0054(3)	0.0102(5)	0.0131(9)
	β_{22}	0.0014(1)	0.0016(1)	0.0011(1)	0.0024(1)	0.0044(2)
	β_{33}	0.0040(2)	0.0031(3)	0.0046(5)	0.0064(3)	0.0108(7)
	β_{12}	0.0001(1)	0.0001(2)	0.0003(1)	0.0002(2)	0.0005(4)
	β_{13}	-0.0002(2)	-0.0001(3)	-0.0001(3)	-0.0005(4)	-0.0002(7)
	β_{23}	0.0005(1)	0.0006(1)	0.0006(2)	0.0011(2)	0.0017(4)
	Beq	0.52(1)	0.50(2)	0.55(2)	0.97(2)	1.56(4)

*$\beta_{13} = \beta_{23} = 0$ *for* Mg, Si, O(1) *and* O(2). *Anisotropic temperature factors have the form* $\exp[-\sum_{i=1}^{3}\sum_{j=1}^{3} h_i h_j \beta_{ij}]$.

**The numbers in parentheses are estimated standard errors (1σ) referring to uncertainty in the last decimal place.

***Beq values are isotropic equivalents of the anisotropic temperature factor coefficients calculated using the expression of Hamilton (1959).

+Total Fe for 12052 olivine includes 0.01 Cr.

range of 2.0° plus the $\alpha_1 - \alpha_2$ dispersion and a scan speed of 1°/minute. A standard reflection was measured every 20 reflections and a 10 second background count was accumulated on both sides of each peak.

After data collection at 24°C, the 12052 olivine crystal was mounted with high temperature cement on a silica glass fiber and placed inside a silica glass capillary which was then evacuated, sealed, and mounted on a standard goniometer head. The crystal was heated to 375 ± 20°C and allowed to equilibrate for about six hours on the Picker diffractometer using a heating device described by Brown *et al* (1973). The 2θ values of 12 reflections were measured at temperature before data collection was begun and submitted to least-squares refinement to determine the cell parameters. Approximately 650 independent intensities were next collected in the same manner as described above for the room temperature data. Following this data set, the above procedure was repeated at 710 ± 25°C. Cell parameters and percent expansion from 24° to 710°C are listed in Table 2. The percent expansion of all parameters is lower than that observed by Kozu, Ueda, and Tsurumi (1934) for Fa_{10} over the range 20–600°C. The percentage volume expansion is also lower than that observed by Rigby, Lovell, and Green (1946) for a series of intermediate Fe-Mg olivines heated from 20–600°C. Optical examination of the crystal after heating showed no evidence of oxidation or breakdown.

All data were reduced in the standard fashion and converted to structure amplitudes. Because of the small size of each crystal (0.10–0.12 mm in diameter) and relatively small linear absorption coefficients, no absorption corrections were applied. Refinement of each data set was initiated using the least-squares program RFINE (L. W. Finger, Geophysical Lab), positional and thermal parameters of a hortonolite refined by Birle *et al* (1968), neutral atomic scattering factors (Doyle and Turner, 1968), and one scale factor. Selected refinement parameters from the final cycle of anisotropic refinement during which a scale factor, a secondary extinction parameter, positional and thermal parameters, and the occupancies of $M(1)$ and $M(2)$ were allowed to vary are listed in Table 3. In all cases unit weights were found to be superior to weights based on counting statistics. The final positional, thermal, and occupancy parameters are given in Table 4. Listings of the final observed and calculated structure factors may be ordered.[2] The orientations and magnitudes of the apparent thermal ellipsoids for each atom (see Table 5), as well as distances, angles, and associated errors, were calculated using Finger's ERROR pro-

[2] To obtain a copy of this material, order NAPS Document Number 02119, by remitting $1.50 for microfiche or $22.10 for photocopies (144 pp.), payable to Microfiche Publications, 305 East 46th Street, New York, N.Y. 10017. Please check the most recent issue of this journal for the current address and prices.

TABLE 5. Magnitudes and Orientations of Thermal Ellipsoids for Five Olivines*

		M1				M2				Si			
OLIVINE	i of r_i	r_i	+a	+b	+c	r_i	+a	+b	+c	r_i	+a	+b	+c
12018(24°C)	1	0.054(2)	20(6)	83(4)	71(5)	0.060(2)	85(7)	175(7)	90	0.049(2)	5(5)	95(5)	90
	2	0.067(2)	71(6)	122(4)	142(5)	0.071(2)	175(7)	95(7)	90	0.065(2)	95(5)	175(5)	90
	3	0.084(2)	95(2)	148(4)	58(4)	0.074(2)	90	90	0	0.071(2)	90	90	0
OG2B(24°C)	1	0.053(3)	17(16)	86(7)	73(15)	0.066(2)	63(13)	153(13)	90	0.047(3)	5(6)	95(6)	90
	2	0.060(3)	73(16)	112(3)	151(10)	0.070(2)	90	90	180	0.065(2)	90	90	180
	3	0.088(2)	93(3)	157(3)	68(3)	0.073(2)	27(13)	63(12)	90	0.067(2)	85(6)	5(6)	90
12052(24°C)	1	0.057(3)	64(9)	55(6)	46(7)	0.042(2)	87(2)	177(2)	90	0.050(2)	74(11)	164(11)	90
	2	0.065(2)	29(9)	118(8)	99(6)	0.071(4)	90	90	180	0.057(2)	164(11)	106(11)	90
	3	0.078(2)	103(5)	132(7)	45(7)	0.079(1)	3(2)	87(2)	90	0.074(4)	90	90	0
12052(375°C)	1	0.085(2)	61(4)	66(2)	40(2)	0.084(2)	88(2)	178(2)	90	0.077(2)	22(15)	112(15)	90
	2	0.103(2)	30(4)	109(3)	112(3)	0.106(2)	90	90	180	0.083(2)	112(15)	158(15)	90
	3	0.124(1)	96(3)	148(2)	59(2)	0.114(2)	2(2)	88(2)	90	0.096(2)	90	90	0
12052(710°C)	1	0.106(3)	36(5)	76(3)	58(4)	0.121(3)	85(11)	175(11)	90	0.090(3)	2(5)	92(5)	90
	2	0.126(3)	54(5)	114(3)	134(4)	0.131(2)	175(11)	95(11)	90	0.114(2)	92(5)	178(5)	90
	3	0.166(2)	93(2)	151(2)	61(2)	0.139(3)	90	90	0	0.123(3)	90	90	0

		O(1)				O(2)				O(3)			
OLIVINE	i of r_i	r_i	+a	+b	+c	r_i	+a	+b	+c	r_i	+a	+b	+c
12018(24°C)	1	0.057(4)	7(6)	97(6)	90	0.069(4)	10(63)	80(63)	90	0.071(3)	33(21)	111(14)	66(14)
	2	0.083(3)	90	90	180	0.072(4)	100(64)	10(64)	90	0.077(3)	57(21)	53(10)	126(12)
	3	0.086(3)	83(6)	7(6)	90	0.086(3)	90	90	0	0.095(2)	92(5)	45(5)	45(5)
OG2B(24°C)	1	0.058(6)	8(6)	98(7)	90	0.068(16)	46(18)	44(18)	90	0.067(4)	50(56)	112(17)	48(44)
	2	0.079(5)	90	90	180	0.078(5)	90	90	180	0.070(4)	40(56)	75(22)	126(46)
	3	0.093(4)	82(7)	8(7)	90	0.081(5)	44(18)	134(18)	90	0.097(3)	87(6)	27(5)	63(5)
12052(24°C)	1	0.064(4)	15(26)	105(26)	90	0.049(5)	85(6)	175(6)	90	0.069(3)	65(10)	144(7)	66(7)
	2	0.071(4)	105(26)	165(26)	90	0.082(3)	175(6)	95(6)	90	0.082(2)	25(10)	69(11)	103(8)
	3	0.087(7)	90	90	0	0.082(8)	90	90	0	0.097(4)	88(9)	62(7)	28(7)
12052(375°C)	1	0.073(5)	10(4)	100(4)	90	0.081(5)	83(6)	7(6)	90	0.093(3)	75(8)	128(4)	42(4)
	2	0.109(4)	90	90	180	0.114(4)	90	90	180	0.110(3)	16(8)	79(8)	100(7)
	3	0.122(4)	80(4)	10(4)	90	0.114(4)	7(6)	97(6)	90	0.127(3)	92(7)	40(4)	50(4)
12052(710°C)	1	0.091(7)	12(6)	102(6)	90	0.118(6)	4(20)	86(20)	90	0.121(5)	31(24)	110(13)	67(20)
	2	0.141(6)	102(6)	168(6)	90	0.132(6)	94(22)	4(22)	90	0.130(5)	60(25)	62(10)	136(15)
	3	0.152(6)	90	90	0	0.137(6)	90	90	0	0.166(4)	86(5)	35(5)	55(5)

* The numbers in parentheses are estimated standard errors (1$\hat{\sigma}$) referring to uncertainty in the last decimal place.

gram. Selected distances uncorrected for thermal motion are listed in Table 6 and selected angles are reported in Table 7. Polyhedral volumes were calculated using a modified version of C. T. Prewitt's unpublished computer program DRLL and are listed in Table 8.

Results and Discussion

Structural Details

The basic structural details of Fe-Mg olivines have been adequately discussed by Birle *et al* (1968). Consequently, we will emphasize structural variations as a function of temperature. Mean $M(1)$–O and $M(2)$–O bond lengths, as well as octahedral volumes, increase slightly (see Tables 6 and 8) in the order 12018 < OG2B < 12052(24°C) as fayalite content increases from Fa_{18}(12018) to Fa_{31} (12052). Mean Si–O distances are constant within this series as is true for a number of transition-metal- and Ca-containing olivines (Brown, 1970). Mean $M(1)$–O and $M(2)$–O bond lengths increase linearly and at essentially the same rate (~0.8% each) in 12052 olivine as a function of temperature over the range studied (Fig. 1). On the other hand, individual and mean Si–O distances are constant within 3 $\hat{\sigma}$ from 24 to 710°C. Other recent high temperature structural studies of silicates (Brown *et al,* 1972; Sueno *et al,* 1972; Cameron *et al,* 1973) also report insignificant variations in Si–O bond lengths. The behavior of mean M–O and Si–O bond lengths with increasing temperature in hortonolite provides a good example of Megaw's (1971) general rule which states that "changes due to temperature in the size or shape of a constituent part of a structure are likely to be small if the same constituent is found

almost undistorted in a variety of different structures. . . . They are likely to be large if the constituent is much modified in size or shape in different structures." The octahedral volumes (Table 8) show expansions of 1.81 percent and 1.94 percent, respectively, for $M(1)$ and $M(2)$ over the temperature range 24 to 710°C, whereas the Si tetrahedron exhibits an insignificant decrease in volume of 0.27 percent over the same range. $M(1)$ and $M(2)$ octahedral angles (see Table 7) show relatively small increases or decreases as a function of temperature; however, mean angles remain constant. Octahedral angles opposite O–O edges shared with the Si-tetrahedron [O(2)–M(1)–O(3′) and O(3)–M(2)–O(3′)] show relatively large decreases whereas the opposite tetrahedral angles [O(2)–Si–O(3) and O(3)–Si–O(3′)] increase slightly with temperature. These changes reflect the strong repulsive interactions between Si and M-cations across the shared polyhedral edges, which appear to increase with increasing temperature. Octahedral and tetrahedral angular changes are also consonant with the predicted relative strengths of the Si–O and M–O bonds.

Octahedral Distortions

Octahedral distortions in a number of transition-metal- and Ca-containing olivines have been discussed in terms of bond-angle strains (Brown, 1970) and bond-angle variance (Robinson, Gibbs, and Ribbe, 1971). Bond-angle variance as defined in the footnote of Table 9 was found to account best for the range of variations from O_h site symmetry commonly observed in silicates. Octahedral angle variances (in degrees) for the $M(1)$ and $M(2)$ octahedra of each olivine in the present study are listed in Table 9. The variance values of 12052 olivine are also plotted as a function of temperature in Figure 1. Several interesting points are worth noting. In each olivine, at room temperature and above, the $M(1)$ octahedron is more distorted than $M(2)$. Octahedral

TABLE 6. Olivine Bond Lengths (Å)*

	12018 (24° C)	0G2B (24° C)	12052 (24° C)	12052 (375° C)	12052 (710° C)
TETRAHEDRON					
** [1] Si-O(1)	1.618(2)	1.619(2)	1.618(2)	1.619(2)	1.622(4)
[1] Si-O(2)	1.659(2)	1.654(2)	1.656(2)	1.659(2)	1.649(4)
[2] Si-O(3)	1.639(1)	1.638(2)	1.638(2)	1.639(2)	1.636(3)
<Si-O>	1.639(2)	1.637(2)	1.638(2)	1.639(2)	1.636(4)
M(1) OCTAHEDRON					
[2] M(1)-O(1)	2.096(1)	2.097(1)	2.101(1)	2.110(1)	2.120(3)
[2] M(1)-O(2)	2.082(1)	2.086(1)	2.087(1)	2.095(2)	2.101(3)
[2] M(1)-O(3)	2.153(1)	2.162(1)	2.165(1)	2.175(1)	2.184(3)
<M(1)-O>	2.110(1)	2.115(1)	2.118(1)	2.127(2)	2.135(3)
M(2) OCTAHEDRON					
[1] M(2)-O(1)	2.186(2)	2.187(2)	2.192(2)	2.208(2)	2.215(4)
[1] M(2)-O(2)	2.067(2)	2.070(2)	2.077(2)	2.080(2)	2.087(4)
[2] M(2)-O(3)	2.066(1)	2.063(1)	2.064(2)	2.074(2)	2.084(3)
[2] M(2)-O(3')	2.236(1)	2.241(2)	2.247(1)	2.255(2)	2.262(3)
<M(2)-O>	2.143(1)	2.144(2)	2.148(2)	2.158(2)	2.166(3)

* uncorrected for thermal motion. The numbers in parentheses represent estimated standard errors ($1\hat{\sigma}$) and refer to the last decimal place.

** the numbers in brackets refer to the multiplicity of the bond.

TABLE 7. Olivine Bond Angles (°)*

	12018(24° C)	0G2B (24° C)	12052 (24° C)	12052 (375° C)	12052 (710° C)
TETRAHEDRON					
**[1] O(1)-Si-O(2)	113.90(8)	113.71(11)	113.71(9)	113.71(12)	113.96(21)
[2] O(1)-Si-O(3)	115.91(5)	115.90(7)	115.92(5)	115.91(7)	115.55(13)
[2] O(2)-Si-O(3)[a]	102.13(5)	120.26(7)	102.15(6)	102.21(7)	102.44(14)
[1] O(3)-Si-O(3')[a]	105.04(8)	105.02(11)	105.18(10)	105.11(11)	105.22(22)
⟨O-Si-O⟩	109.17(6)	109.18(9)	109.17(7)	109.18(9)	109.19(17)
M(1) OCTAHEDRON					
[2] O(1)-M(1)-O(3)[b]	84.92(5)	84.85(7)	84.95(6)	84.92(7)	84.79(13)
[2] O(1)-M(1)-O(3')	95.08(5)	95.15(7)	95.05(6)	95.08(7)	95.21(13)
[2] O(1)-M(1)-O(2)[b]	86.56(4)	86.52(6)	86.56(4)	86.54(6)	86.46(10)
[2] O(1)-M(1)-O(2')	93.44(4)	93.48(6)	93.44(4)	93.46(6)	93.54(10)
[2] O(2)-M(1)-O(3)	105.45(5)	105.80(7)	105.90(6)	106.12(7)	106.60(13)
[2] O(2)-M(1)-O(3')[a]	74.55(5)	74.20(7)	74.10(6)	73.88(7)	73.40(13)
⟨O-M(1)-O⟩	90.00(5)	90.00(7)	90.00(5)	90.00(7)	90.00(12)
M(2) OCTAHEDRON					
[2] O(1)-M(2)-O(3)	80.89(4)	80.91(6)	80.94(5)	80.81(6)	80.81(11)
[2] O(1)-M(2)-O(3")[b]	91.17(4)	91.19(5)	91.21(4)	91.10(6)	91.00(10)
[2] O(2)-M(2)-O(3)	96.61(5)	96.56(6)	96.54(5)	96.84(7)	97.14(12)
[2] O(2)-M(2)-O(3"')	90.57(4)	90.56(5)	90.52(4)	90.51(6)	90.40(10)
[1] O(2)-M(2)-O(3')[a]	71.17(6)	70.88(8)	70.75(8)	70.49(8)	70.16(16)
[2] O(3)-M(2)-O(3")	88.48(2)	88.31(3)	88.34(3)	88.33(3)	88.25(7)
[1] O(3)-M(2)-O(3"')	111.20(6)	111.84(9)	111.92(8)	112.17(9)	112.64(17)
⟨O-M(2)-O⟩	89.82(4)	89.82(6)	89.81(5)	89.82(6)	89.83(11)

*The numbers in parentheses represent estimated standard errors ($1\hat{\sigma}$) and refer to the last decimal place.

**The numbers in brackets refer to the multiplicity of the angle.

[a]Angle opposite O-O polyhedral edge shared between an octahedron and tetrahedron.

[b]Angle opposite O-O polyhedral edge shared between two octrahedra.

distortion increases as a function of temperature and, over the range studied, $M(1)$ distortion increases at a faster rate than $M(2)$ distortion with increasing temperature. The observed increase in octahedral distortion with temperature suggests that the approximately hexagonal closest-packed framework of oxygen anions characterizing olivine becomes less ideally h.c.p. as a function of temperature. Our data contradict the suggestion by Eliseev (1958) that olivine has a tendency toward increased symmetry on heating. The intensity changes, splitting, and coalescence of peaks that he observed on heating Fa_{13} powder are probably due to oxidation of Fe^{2+} and breakdown to other phases.

The observed differential octahedral distortions help in interepreting recent Mössbauer spectra of olivines by Malysheva, Kurash, and Ermakov (1969), Bush, Hafner, and Virgo (1970), Finger and Virgo (1971), and Virgo and Hafner (1972). Earlier Mössbauer studies of olivines at room temperature were unsuccessful at resolving the two doublets caused by Fe^{2+} on the $M(1)$ and $M(2)$ sites. However, when heated in the range 200–500°C, the

TABLE 8. Comparison of Polyhedral Volumes (Å)^3 for Five Olivines

Polyhedron	12018 (24° C)	0G2B (24° C)	12052 (24° C)	12052 (375° C)	12052 (710° C)
SiO_4	2.224	2.218	2.222	2.224	2.216
$M(1)O_6$	12.019	12.074	12.143	12.252	12.371
$M(2)O_6$	12.606	12.615	12.708	12.834	12.955

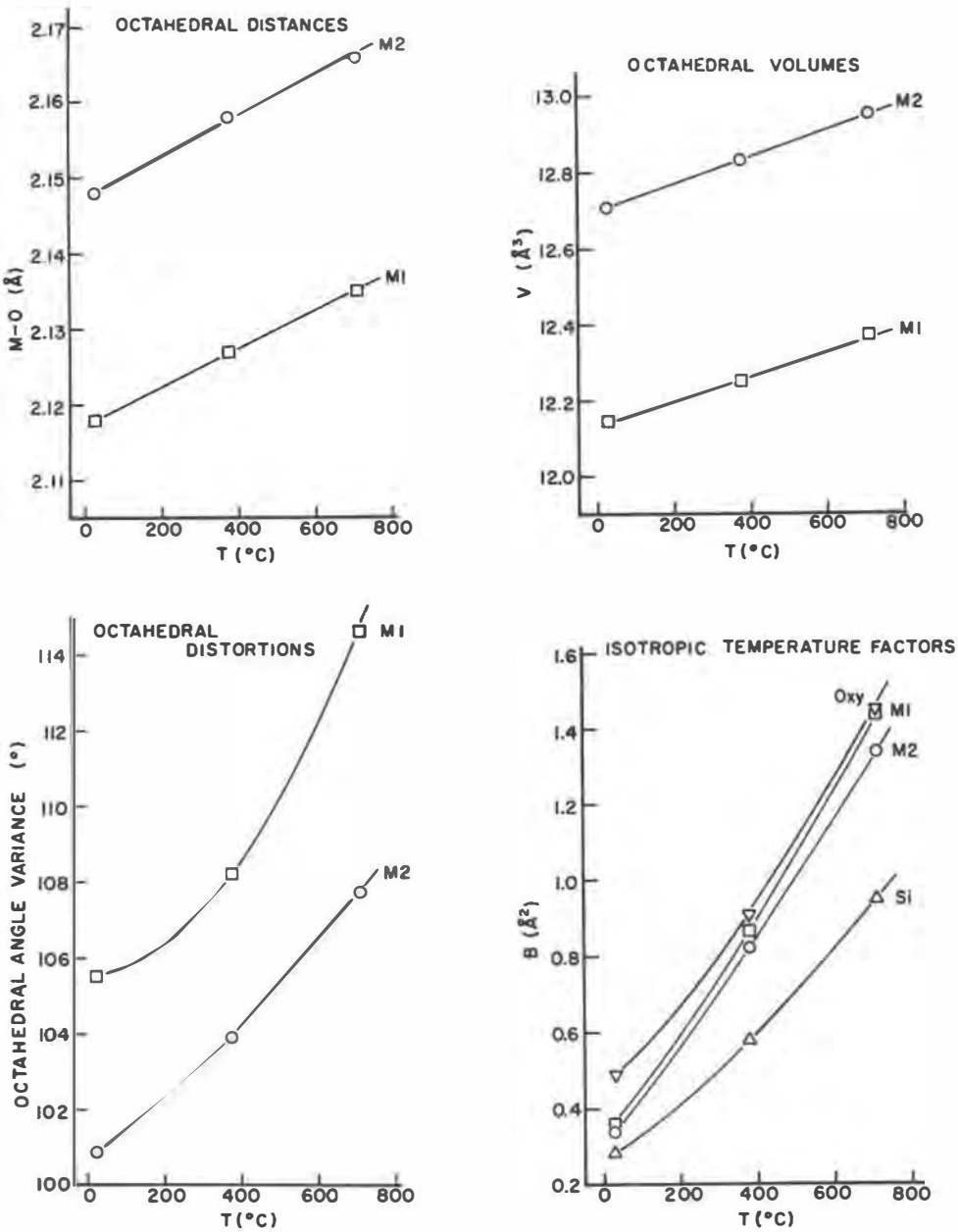

FIG. 1. Variation of mean octahedral metal-oxygen distances (M–O), octahedral volumes (V), octahedral angle variances and isotropic equivalent temperature factors (B) of 12052 olivine as a function of temperature. Data for each plot are listed in Tables 6, 8, 9, and 4, respectively.

doublets are readily resolvable. This resolution at temperature may be explained by the observed differential increase in octahedral distortion with temperature. Because quadrupole splitting is thought to vary inversely with site distortion (see Virgo and Hafner, 1969 and others), the inner doublet in olivine spectra may be assigned to Fe^{2+} on the more distorted $M(1)$ site. Earlier assignments were based on X-ray site population data determined at room temperature. Moreover, the strong temperature dependence of quadrupole splittings reported by Shenoy, Klavius, and Hafner (1969) for orthopyroxenes may result from a similar differential change in polyhedral distortions with increasing temperature.

TABLE 9. Octahedral Distortions* in Five Olivines

	12018 (24° C)	0G2B (24° C)	12052 (24° C)	12052 (375° C)	12052 (710° C)
σ^2_θ(M1)	104.83	100.49	105.51	108.23	114.63
σ^2_θ(M2)	100.28	96.85	100.88	103.94	107.77
% DIFFERENCE	4.34	3.62	4.38	3.96	5.98

* σ^2_θ (OCT) $= \sum_{i=1}^{12} (\theta - 90°)^2/11$ [Robinson *et al.*, 1971]

Thermal Parameters

The isotropic equivalents, Beq, of the anisotropic temperature factor coefficients from the three room temperature refinements (see Table 4) are in good agreement with those reported for the Fe-Mg olivines (Birle *et al,* 1968; Finger, 1970). Beq values of $M(1)$, $M(2)$, Si, and the average O in 12052 olivine are plotted as a function of temperature in Figure 1 and show smooth increases in all cases. The anisotropy of apparent thermal motion in 12052 (Table 5), as estimated by the percentage difference between the minimum and maximum displacements, increases for $M(1)$ and O(1) and decreases in all other cases as a function of temperature. The decrease in anisotropy of $M(2)$ is related to the large increase in apparent thermal motion parallel to *b*, which probably includes the effects of positional disorder. The increase and decrease in anisotropy of the $M(1)$ and $M(2)$ cations, respectively, may also be related to the differential distortions of the two polyhedra with increasing temperature.

Fe/Mg Distributions in Olivines

The results of octahedral occupancy refinements, carried out using explicit chemical constraints, are listed in Table 4 and compared with other recent occupancy determinations of olivines in Table 10. The calculated distribution coefficients, K_D, suggest that OG2B olivine is disordered [$K_D = 1.02(4)$] and that olivines 12018 [$K_D = 1.15(3)$] and 12052 [$K_D = 1.19(3)$] are significantly ordered, with Fe^{2+} preferentially occupying the $M(1)$ site. The observed partial anti-ordering of Fe and Mg agrees with the recent results obtained by Finger (1970) and Finger

TABLE 10. Comparison of Fe/Mg Distribution for Selected Olivines

OLIVINE	R	B(M1)	B(M2)	M1 OCCUPANCY[1]		M2 OCCUPANCY[1]			$\hat{\sigma}$	K_D[2]
				Mg	Fe'	Mg	Fe'	Ca		
0G2B	0.029	0.37(2)[3]	0.38(1)	0.708	0.292	0.712	0.288	—	0.003	1.02(4)
12018[4]	0.023	0.38(1)	0.38(1)	0.814	0.186	0.826	0.164	0.010	0.002	1.15(3)
12018[5]	0.035	0.64(2)	0.64(2)	0.656	0.344	0.684	0.316	—	0.004	1.14(4)
12018[6]	0.038	0.68(2)	0.76(2)	0.675	0.325	0.665	0.335	—	0.003	0.96(3)
12052(24° C)	0.025	0.36(2)	0.34(2)	0.675	0.325	0.705	0.285	0.010	0.003	1.19(3)
12052(375° C)	0.031	0.87(2)	0.82(2)	0.677	0.323	0.703	0.287	0.010	0.003	1.17(3)
12052(710° C)	0.057	1.44(3)	1.34(3)	0.670	0.330	0.710	0.280	0.010	0.005	1.25(6)
10020[7]	0.048	0.64(2)	0.64(2)	0.729	0.271	0.734	0.258	0.008	0.005	1.06(6)
C15-64[7]	0.026	0.46(2)	0.49(2)	0.477	0.523	0.503	0.490	0.007	0.004	1.13(4)
B1[8]	0.038	0.56(2)	0.47(2)	0.807	0.192	0.846	0.147	0.007	0.004	1.37(4)

[1] Fe' refers to Fe plus small quantities of other elements such as Mn.
[2] K_D=[Mg(M2) Fe(M1)]/[Mg(M1) Fe(M2)] for the exchange reaction Mg(M1)+Fe(M2)⇌Mg(M2)+Fe(M1). $\hat{\sigma}$ of K_D was calculated using the propagation of error technique. Ca assumed fixed in M2.
[3] Numbers in parentheses are estimated standard errors ($1\hat{\sigma}$) referring to the last decimal place.
[4] Correct chemistry and unit weights
[5] Incorrect chemistry and unit weights
[6] Incorrect chemistry and weights based on counting statistics
[7] From Finger (1970)
[8] From Finger and Virgo (1971)

and Virgo (1970) on lunar and terrestrial olivines (see Table 10) but is at variance with the suggestion by Burns (1970a) that Fe^{2+} is slightly enriched in the $M(2)$ site of some Fe-Mg olivines. There is no evidence from the data presented in Table 10 to support the claim made by Wenk and Raymond (1971) that the ordering of Fe^{2+} on $M(1)$ increases with increasing Fe content.

Before the probe analysis of 12018 olivine was completed, the incorrect composition Fa_{33} was used in the least-squares refinement of X-ray data (correct composition is Fa_{18}). It is surprising, and somewhat sobering, that the R-factor (0.035) and estimated occupancy errors (± 0.004) are well within the acceptable range and that K_D[1.14(4)] is not significantly different from that obtained in the refinement with correct chemistry (see Table 10). Moreover, when weights based on counting statistics were used in place of unit weights, the refinement using incorrect chemistry resulted in a significantly different K_D value [0.96(3)] which suggested slight relative enrichment of Fe^{2+} on $M(2)$. Again, the resulting R-factor (0.038) and occupancy error (± 0.003) are quite acceptable when compared with other proper refinements of olivine. The relatively high values of the isotropic temperature factors, B, for $M(1)$ and $M(2)$ were the only clues that something was amiss (see Table 10). It is important therefore to ensure that the correct chemistry is known, preferably by probe analysis of the crystal used in the collection of intensity data.

The degree of octahedral distortion is one of several factors considered to be important in determining the amount of crystal field stabilization energy that a transition metal cation such as Fe^{2+} receives in an octahedral site in silicates. Using the site-distortion criterion and assuming that the $M(2)$ octahedron is more distorted than $M(1)$, Burns (1970b) predicted that Fe^{2+} should preferentially occupy the $M(2)$ site in olivines. The high temperature structural data from the present study indicate that the $M(1)$ site is more distorted than $M(2)$ and that the difference becomes greater with increasing temperature. Therefore, Burns' prediction may be rejected. Furthermore, these results show a possible danger in establishing or assessing cation ordering criteria in silicates without a knowledge of the structure at temperatures approaching (or above) those at which cation diffusion takes place.

Recent heating experiments on a more Fe-rich specimen of 12018 olivine at a temperature of 1155°C (for seven days) followed by Mössbauer spectra (Virgo and Hafner, 1972) suggest that significant cation diffusion did take place at this temperature. When a more Fe-rich, partially ordered specimen was heated at 1055°C (for five days), no change in K_D was observed by Virgo and Hafner. However, Moore and Evans (1967) have inferred from a detailed microprobe study of olivine phenocrysts from the Makaopuhi Lava Lake, Hawaii, that interdiffusion of Fe and Mg may continue to as low as 800°C, given sufficient time. The lack of significant ordering in the metamorphic olivine OG2B is not surprising in light of these observations coupled with the high temperature olivine data for 12052. A possible explanation for the random arrangement of Fe and Mg is that differences in site distortion and size are not significant enough to promote relative enrichment of Fe^{2+} on $M(1)$ at the estimated temperature of metamorphism (~650°C) even though cooling was extremely slow. The cooling history of 12052 olivine, discussed in the section on experimental details, is thought to entail an early, slow cooling, high temperature stage during which olivine crystallization occurred, followed by a second, fast cooling stage from high temperature upon eruption onto the lunar surface. The relatively high degree of order [$K_D = 1.19(3)$] is consistent with such a proposed history. One of the most surprising results of this study involves a comparison between the X-ray site population data (this study) and the Mössbauer site population data for samples of 12018 olivine. The more Fe-rich sample used in the Mössbauer study (Fa_{33}) by Finger and Virgo (1971) was found to have the highest K_D value [1.75] yet reported for an Fe-Mg olivine, whereas the less Fe-rich sample used in this study (Fa_{18}) was found to be significantly less ordered [$K_D = 1.15(3)$]. If these samples came from the same rock, as is believed to be the case, an anomalous situation presents itself. The early crystallizing Mg-rich crystals are less ordered than the late crystallizing Fe-rich crystals.

Further studies of Fe-Mg olivines as a function of temperature and composition are needed to explain the anomaly mentioned above as well as the temperature dependence of Fe/Mg distributions in olivines. Additional high temperature structural studies on olivines as well as on other Fe/Mg silicates are necessary in order to establish proper ordering criteria based on cation/site sizes and site distortions. Perhaps a more useful result of these studies will be data on differential structural expansion as a func-

tion of temperature. This should permit determination of possible diffusion paths between non-adjacent sites in a silicate.

Acknowledgments

We wish to thank Dr. David Virgo (Geophysical Lab) and Professor Peter Robinson (Univ. Massachusetts) for providing samples of olivine, and gratefully acknowledge Professor A. E. Bence (Stony Brook) for performing the microprobe analyses of the three crystals studied. Thanks are also extended to Professors G. V. Gibbs (VPISU) and D. R. Waldbaum (Princeton) for critically reviewing the manuscript. This research was supported by NSF Grant GA-12973 and NASA Grant NGL 33-015-130. The secretarial staff of the Department of Geological and Geophysical Sciences at Princeton is thanked for their patient typing of the manuscript.

References

Bell, P. M. (1971) Analysis of olivine crystals in Apollo 12 rocks. *Carnegie Inst. Year Book,* **69,** 228–229.

Belov, N. V., E. N. Belova, N. H. Andrianov, and P. F. Smirnova (1951) Determination of the parameters in the olivine (forsterite) structure with the harmonic three-dimensional synthesis. *Dokl. Akad. Nauk S.S.S.R.* **81,** 399–402.

Bence, A. E., J. J. Papike, and C. T. Prewitt (1970) Apollo 12 clinopyroxenes: chemical trends. *Earth Planet. Sci. Lett.* **8,** 393–399.

———, ———, and D. H. Lindsley (1971) Crystallization histories of clinopyroxenes in two porphyritic rocks from Oceanus Procellarum. *Proc. Second Lunar Sci. Conf.* **1,** 559–574.

Birle, J. D., G. V. Gibbs, P. B. Moore, and J. V. Smith (1968) Crystal structures of natural olivines. *Amer. Mineral.* **53,** 807–824.

Brown, G. E. (1970) *Crystal chemistry of the olivines.* Ph.D. Thesis, Virginia Polytechnic Institute and State University, Blacksburg, Virginia.

———, C. T. Prewitt, J. J. Papike, and S. Sueno (1972) A comparison of the crystal structures of low and high pigeonite. *J. Geophys. Res.* **77,** 5778–5789.

———, S. Sueno, and C. T. Prewitt (1973) A new single-crystal heater for the precession camera and four-circle diffractometer. *Amer. Mineral.* **58,** 698–704.

Burns, R. G. (1970a) Crystal field spectra and evidence of cation ordering in olivine minerals. *Amer. Mineral.* **55,** 1608–1632.

——— (1970b) *Mineralogical Applications of Crystal Field Theory.* Cambridge University Press, Cambridge, England.

Bush, W. R., S. S. Hafner, and D. Virgo (1970) Some ordering of iron and magnesium at the octahedrally coordinated site in a magnesium-rich olivine. *Nature,* **227,** 1339–1341.

Cameron, M., S. Sueno, C. T. Prewitt, and J. J. Papike (1973) High-temperature crystal chemistry of acmite, diopside, hedenbergite, jadeite, spodumene, and ureyite. *Amer. Mineral.* **58,** 594–618.

Doyle, P. A., and P. S. Turner (1968) Relativistic Hartree-Fock X-ray and electron scattering factors. *Acta Crystallogr.* **A24,** 390–397.

Eliseev, E. N. (1958) New data on the crystal structure of olivine. *Soviet Physics-Crystallogr.* **3,** 163–170.

Finger, L. W. (1969) Determination of cation distributions by least-squares refinement of single-crystal X-ray data. *Carnegie Inst. Year Book,* **67,** 216–217.

——— (1971) Fe/Mg ordering in olivines. *Carnegie Inst. Year Book,* **69,** 302–305.

———, and D. Virgo (1971) Confirmation of Fe/Mg ordering in olivines. *Carnegie Inst. Year Book,* **70,** 221–225.

Hamilton, W. C. (1959) On the isotropic temperature factor equivalent to a given anisotropic temperature factor. *Acta Crystallogr.* **12,** 609–610.

Hanke, K. (1965) Beitrage Zu Kristallstrukturen vom Olivin-typ. *Beitr. Mineral. u. Petrogr.* **11,** 535–558.

Kozu, S., J. Ueda, and S. Tsurumi (1934) Thermal expansion of olivine. *Proc. Imp. Acad. Japan,* **10,** 83–86.

Kushiro, I., Y. Nakamura, K. Kitayama, and S. Akimoto (1971) Petrology of some Apollo 12 crystalline rocks. *Proc. Second Lunar Sci. Conf.* **1,** 481–495.

Malysheva, T. V., V. V. Kurash, and A. N. Ermakov (1969) Study of isomorphic replacement of magnesium and iron (II) in olivines by Mössbauer γ-resonance spectroscopy. *Geokhimiya,* **11,** 1405–1408.

Megaw, H. D. (1971) Crystal structures and thermal expansion. *Mat. Res. Bull.* **6,** 1007–1018.

Moore, J. G., and B. W. Evans (1967) The role of olivine in the crystallization of the prehistoric Makaopuhi Tholeiitic Lava Lake, Hawaii. *Contrib. Mineral. Petrology,* **15,** 202–223.

Papike, J. J., A. E. Bence, G. E. Brown, C. T. Prewitt, and C. H. Wu (1971) Apollo 12 clinopyroxenes: exsolution and epitaxy. *Earth Planet. Sci. Lett.* **10,** 307–315.

Rigby, G. R., G. B. H. Lovell, and A. T. Green (1946) The reversible thermal expansion and other properties of some magnesian ferrous silicates. *Trans. Brit. Ceram. Soc.* **45,** 237–250.

Robinson, K., G. V. Gibbs, and P. H. Ribbe (1971) Quadratic elongation: a quantitative measure of distortion in coordination polyhedra. *Science,* **172,** 567–570.

Shenoy, G. K., G. M. Kalvius, and S. S. Hafner (1969) Magnetic behavior of the $FeSiO_3$-$MgSiO_3$ orthopyroxene system from NGR in ^{57}Fe. *J. Appl. Phys.* **40,** 1314–1316.

Sueno, S., J. J. Papike, C. T. Prewitt, and G. E. Brown (1972) Crystal structure of high cummingtonite. *J. Geophys. Res.* **77,** 5767–5777.

Virgo, D., and S. S. Hafner (1969) Fe^{2+}-Mg order-disorder in heated orthopyroxenes. *Mineral. Soc. Amer. Spec. Pap.* **2,** 67–81.

———, and ——— (1972) Temperature-dependent Mg, Fe distribution in a lunar olivine. *Earth Planet. Sci. Lett.* **14,** 305–312.

Wenk, H. R., and K. N. Raymond (1971) Crystal structure refinements of four magnesium-rich olivines (abstr.). *Geol. Soc. Amer. Abstr. Programs,* **3,** 748–749.

Manuscript received, February 7, 1973;
accepted for publication, March 13, 1973.